

## Theoretical and Experimental Analyses of Heat Transfer in a Flat-Plate Solar Collector

Bukola Olalekan BOLAJI<sup>1</sup> and Israel ABIALA<sup>2</sup>

<sup>1</sup>*Department of Mechanical Engineering, College of Engineering, Federal University of Agriculture, Abeokua, Nigeria*

<sup>2</sup>*Department of Mathematics, College of Natural sciences, Federal University of Agriculture, Abeokua, Nigeria*

(Corresponding author; e-mail: [bobbolaji2007@yahoo.com](mailto:bobbolaji2007@yahoo.com))

*Received: 1 January 2012, Revised: 12 March 2012, Accepted: 5 August 2012*

### Abstract

In this paper, the heat transfer in a flat-plate solar collector with water tubes spreading across its width was analyzed. The performances of the system both theoretically and experimentally were evaluated and compared. The theoretical results obtained agreed well with the experimental results, except that a slight higher deviation of heat loss was obtained in the experimental analysis and low solar radiation in the morning and late afternoon affects the system. An average heat loss coefficient of  $0.68 \text{ W/m}^2 \cdot ^\circ\text{C}$  was obtained in the experimental analysis, while  $0.65 \text{ W/m}^2 \cdot ^\circ\text{C}$  was obtained in the theoretical analysis. The collector efficiency was high around the mid-day when the collector receives the highest energy and the useful heat rate was at its maximum. The results also reveal that the performance of the solar collector depends much on the heat rate. The collector efficiency increases as the heat rate increases until a maximum efficiency of 72.2 % was reached at optimum heat rate of 785 W.

**Keywords:** Experimental, flat-plate, heat transfer, performance, solar collector

### Introduction

Improvements in quality of life and rapid industrialization in many countries are increasing energy demand significantly, and the potential future gap between energy supply and demand is predicted to be large [1]. Therefore, the issue of sustainable development is gaining steady momentum. The renewable energies being inherently sustainable and environment-friendly are gaining popularity. All developed countries and many developing countries have included renewable energies as important sources of energy in their energy planning [2,3]. In February 2008, the UK Government established a review of current and future targets to reduce the UK's CO<sub>2</sub> emissions. The new climate change bill [4] set a target reduction of at least 60 % by 2050. Low and Zero Carbon Technologies (LZCT) have the potential to meet the important concern with

respect to economical, ecological and social issues of sustainable development [5].

Among the various type of clean energy, special attention has been given to solar energy because it is freely available. As worldwide energy reserves have continued to diminish, the incentive to develop solar energy systems has increased. Research on applications of solar energy technologies have as a consequence expanded rapidly, exploiting the abundant, free and environmentally benign characteristics of solar energy. The utilization of solar energy is important in developing nations where electrical energy is expensive and energy production is too low to meet requirements. Solar energy is an ideal alternative source of energy because it is abundant, inexhaustible and non-polluting. It is a free-gift of nature not subjected to future depletion, unlike oil

reserves and mineral deposits, which are subject to depletion in the near future [6,7].

Some solar thermal systems, such as solar water heaters, air heaters, cookers, dryers and distillation devices, have advanced notably in decades in terms of efficiency and reliability. Efficiencies of these devices typically range from about 40 to 60 % for low- and medium-temperature applications [8]. The solar collector is essentially the most important component of the equipment, which transforms radiant energy to heat energy and finally transfers this heat to a working fluid for an end use system. There are two basic types of solar collectors: the concentrating and the flat-plate solar collectors. The concentrating collector may be of tracking type or non-tracking type, depending on the required range of temperature. They operate only with direct beam radiation from the sun and they are only effective on clear sky days. The flat-plate collector has the advantage of absorbing both beam and diffused radiation, and therefore, still functions when radiation is cut-off by the cloud [9,10].

The optimum direction of the flat-plate collector is usually fixed and is designed for applications requiring energy delivered at temperatures less than 100 °C above the ambient temperature [11,12]. The most usual configuration of a domestic solar hot water system with heat pipes is a flat-plate welded on the heat pipes, where the cooling water passes through and removes heat from the collector. The water circulates between the collector and the thermal reservoir, where the heat absorbed in the flat-plate collector is stored [13]. The flat-plates are mounted inside a box cover at the top with transparent glass. This arrangement is made to minimize the thermal losses. Thermosyphon domestic solar water heaters with flat-plate collectors have been widely installed in residential and office buildings for water and space heating due to their reliable performance, low cost, minimal need for maintenance and easy to integrate with the facade of buildings [14].

Numerous studies have been performed on flat-plate solar water heating systems. Rommel and Mook [15] investigated a flat-plate solar collector of rectangular narrow ducts absorber type. In their consideration of the thermal heat gained by the collector, they concluded that considerable improvement in thermal performance of the

collector can be achieved with rectangular ducts absorber, but also with extra cost for its increased consumption of electric pumping energy.

Ismail and Abogderah [16] carried out a comparative study between theoretical predictions and experimental results of a flat-plate solar collector with heat pipes. The theoretical model for the heat pipe solar collector was based upon the method by Duffie and Beckman [17], but modified to use heat pipes for energy transport. Their results revealed that the instantaneous efficiencies of the heat pipe solar collector are lower than the conventional collector in the morning and higher when the heat pipes reach their operating temperatures.

Facao and Oliveira [18] analyzed the thermal behaviors of a flat-plate heat pipe solar collector experimentally. The major simplification was that the temperature in the heat pipe was considered to be uniform and equal to the saturation temperature. Their results showed a collector optical efficiency of 64 % and overall loss coefficient of 5.5 W/m<sup>2</sup>K, for a non-selective surface coating.

Various studies reviewed above have shown the effects of various collector absorber designs on the heat transfer and the performance of the solar water heating system. In this study, heat transfer in a solar collector with fluid channel tubes spreading across its width was investigated theoretically and experimentally. The governing equations of the collector and connecting pipes are presented. The mathematical models presented in this paper go beyond the energy balance equations and add heat transfer equations of collector's components. Theoretical equations were used for evaluating the thermal efficiency of the collector, outlet water temperature and various heat losses from the system. The manufacturing simplicity and absence of moving parts make it an interesting technological solution for production of hot water in rural areas.

## Materials and methods

### Collector overall heat transfer coefficient

A schematic diagram of a flat-plate solar collector with water pipes is shown in **Figure 1**. In order to calculate the overall heat loss coefficient (conductance) a detailed analysis of all heat losses in the collector is required. At some typical location on the absorber plate where temperature is  $T_p$ , the amount of solar energy absorbed per unit

area by the plate is represented by “I”. This absorbed energy is distributed to losses through the top, back, edges and to useful energy gain. The energy loss through the back of the collector is due to the resistance to heat flow through the insulation,  $U_b$ , therefore,

$$U_b = \frac{k}{z} \quad (1)$$

where,  $k$  = insulation thermal conductivity ( $\text{W/m}\cdot^\circ\text{C}$ )

$z$  = insulation thickness (m)

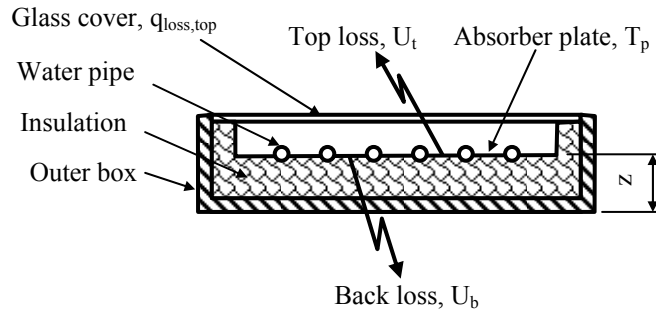


**Figure 1** A schematic diagram of a flat-plate solar collector with water pipes.

The loss coefficient for the top surface is the results of convection and radiation between parallel plates. The heat transfer between the plate at temperature  $T_p$  and the cover glass at temperature  $T_g$  is equal to the heat lost to the surroundings from the cover glass. The loss through the top per unit area ( $q_{\text{loss,top}}$ ) is:

$$q_{\text{loss,top}} = h_{pg}(T_p - T_g) + \frac{\sigma(T_p^4 - T_g^4)}{\frac{1}{\varepsilon_p} + \frac{1}{\varepsilon_g} - 1} \quad (2)$$

where  $h_{pg}$  = heat transfer coefficient between plate and cover glass ( $\text{W/m}^2\cdot^\circ\text{C}$ );  $T_p$  = temperature of the collector absorber plate ( $^\circ\text{C}$ );  $T_g$  = temperature of the collector cover glass ( $^\circ\text{C}$ );  $\sigma$  = Stefan Boltzman constant;  $\varepsilon_p$  = emittance of the absorber plate;  $\varepsilon_g$  = emittance of the cover glass.

If the radiation term is linearized, the radiation heat transfer coefficient can be used and the heat loss becomes:

$$q_{\text{loss,top}} = (h_{pg} + h_{R,pg})(T_p - T_g) \quad (3)$$

where,  $h_{R,pg}$  = radiation heat transfer coefficient between cover glass and surrounding ( $\text{W/m}^2\cdot^\circ\text{C}$ ). Substitution of Eq. (3) in Eq. (2) yields:

$$h_{R,pg} = \frac{\sigma(T_p + T_g)(T_p^2 + T_g^2)}{\frac{1}{\varepsilon_p} + \frac{1}{\varepsilon_g} - 1} \quad (4)$$

The resistance to heat flow between the plate and cover glass ( $R_{pg}$ ,  $\text{m}^2\cdot^\circ\text{C/W}$ ) can be expressed as:

$$R_{pg} = \frac{1}{h_{pg} + h_{R,pg}} \quad (5)$$

The radiation resistance from the cover glass accounts for radiation exchange with the surroundings at  $T_s$ . Therefore, the radiation heat transfer coefficient between the cover glass and the surroundings ( $h_{R,gs}$ ,  $\text{W/m}^2\cdot^\circ\text{C}$ ) can be written as:

$$h_{R,gs} = \frac{\varepsilon_g \sigma (T_g + T_s)(T_g^2 + T_s^2)(T_g - T_s)}{(T_g - T_s)} \quad (6)$$

The resistance to the surroundings ( $R_{gs}$ ,  $\text{m}^2\cdot^\circ\text{C/W}$ ) can be expressed as:

$$R_{gs} = \frac{1}{h_w + h_{R,gs}} \quad (7)$$

For a single glass cover system the top loss coefficient from the collector plate to ambient ( $U_t$ ,  $\text{W/m}^2\cdot^\circ\text{C}$ ) is:

$$U_t = \frac{1}{R_{pg} + R_{gs}} \quad (8)$$

Substitution of Eqs. (5) and (7) in Eq. (8) yields:

$$U_t = \left( \frac{1}{h_{pg} + h_{R,pg}} + \frac{1}{h_w + h_{R,gs}} \right)^{-1} \quad (9)$$

Therefore, the overall loss coefficient ( $U_L$ ,  $W/m^2 \cdot ^\circ C$ ) is found by adding together the top and back loss coefficients, Eqs. (1) and (9):

$$U_L = U_t + U_b \quad (10)$$

### Heat transfer in the flat-plate solar collector

The heat gained by the collector ( $Q_c$ ) can be expressed by the following relationship [13,19]:

$$Q_c = F_R A_c [\alpha \tau I - U_L (T_{ci} - T_a)] \quad (11)$$

where  $F_R$  = collector heat removal factor;  $A_c$  = area of transparent cover ( $m^2$ );  $I$  = incident solar radiation ( $W/m^2$ );  $U_L$  = overall heat loss for the collector ( $W/^\circ C$ );  $\alpha$  = solar absorptance;  $\tau$  = transmittance;  $T_{ci}$  = collector inlet water temperature ( $^\circ C$ );  $T_a$  = ambient air temperature ( $^\circ C$ ).

The useful heat gain by the fluid ( $Q_u$ ) is given as [14]:

$$Q_u = m C_p (T_{co} - T_{ci}) \quad (12)$$

where  $m$  = mass flow rate of fluid ( $kg/s$ );  $C_p$  = specific heat capacity of fluid ( $kJ/kg \cdot ^\circ C$ );  $T_{co}$  = collector outlet water temperature ( $^\circ C$ ).

### Thermal efficiency of solar heating systems

Collector efficiency of solar heating systems ( $\eta_c$ ) is the ratio of useful heat gain by the collector to solar radiation incident on the absorber of solar collector [20], therefore,

$$\eta_c = \frac{Q_c}{A_c I} \quad (13)$$

Substitution of Eq. (11) in Eq. (13) yields:

$$\eta_c = F_R \left[ \alpha \tau - U_L \frac{(T_{ci} - T_a)}{I} \right] \quad (14)$$

Since  $F_R$ ,  $\alpha \tau$  and  $U_L$  are constant, therefore,

$$\eta_c \propto \frac{(T_{ci} - T_a)}{I} \quad (15)$$

The expression  $(T_{ci} - T_a)/I$  is referred to as the collector performance coefficient. In the theoretical analysis, the performance of the system is predicted by solving the mathematical equations by varying the values of the following parameters: ambient air temperature ( $T_a$ ), collector inlet water temperature ( $T_{ci}$ ) and solar radiation ( $I$ ).

### The experimental setup

The top view of the flat-plate solar collector is shown in **Figure 2**. The absorber steel plate of the solar collector was formed like a corrugated sheet to accommodate the water pipes and headers in the grooves to maintain good contacts with the pipes (**Figure 2**). Each pipe is 1 m long and has an inner diameter of 17 mm and outer diameter of 20 mm. The pipes are placed close together horizontally with a space of 83 mm in between and welded at both ends to the header pipes of 22 mm internal diameter, 25 mm outside diameter and 700 mm long each.

The absorber-water pipe assembly formed an inner box, which in turn is mounted in an outer box, the space between the inner box and outer box is filled with wood shavings as an insulating material. The front surface of the box is then covered with 4 mm thick clear plain glass and the air gap between the plate and the glass cover is 76 mm. The overall dimensions of flat-plate solar collector are 1,130 mm  $\times$  830 mm  $\times$  190 mm and the effective glazing area is 0.7  $m^2$ . The absorbing surfaces were painted with matt black to increase their rate of absorbing energy. **Figure 3** shows the experimental set-up of the solar water heating system.

The water inlet and outlet temperatures for the collector and ambient temperature were measured with mercury thermometers with a precision of 0.1  $^\circ C$ . The solar radiation was measured with a Kipp and Zonen pyranometer, with an accuracy of  $\pm 5\%$ . The system was tested for 12 days in the month of November 2005, and readings were taken at intervals of one hour between 8.00 h and 18.00 h each day. The collector was fed with water from the bottom of the storage tank. The water inlet temperature obtained ranges from 30.0 to 42.5  $^\circ C$ . The data obtained were used to compute the system performance parameters using Eqs. (10), (11), (12) and (14).

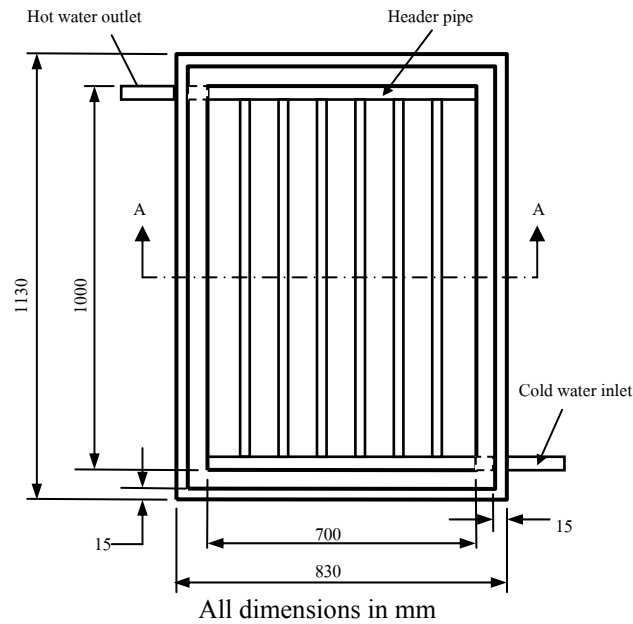


**Figure 2** Top view of flat-plate solar collector.

### Results and discussion

A typical day hourly variation of ambient temperature, collector outlet water temperature and solar radiation is shown in **Figure 4**. The results show that the maximum water temperature obtained is a function of solar radiation and ambient air. The energy received by the collector was high around mid-day during high solar radiation, but it was low in the morning and late afternoon due to the low solar radiation. Therefore,

the maximum temperature occurred after the peak solar radiation. A maximum water temperature of 83.5 °C was obtained, while the maximum ambient temperature for the same day was 34.5 °C. This shows that the hot water temperature was 49 °C higher than the ambient temperature around 14.00 h of the day. The high temperature difference obtained was as a result of proper insulation of the system.



Figure 3 The experimental set-up of the solar water heating system.

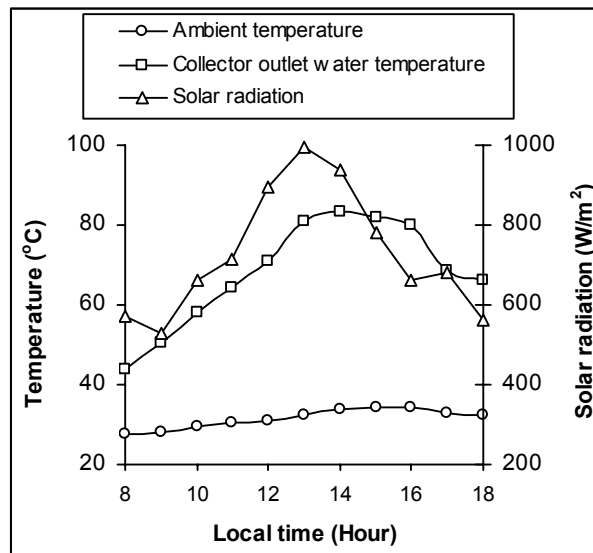
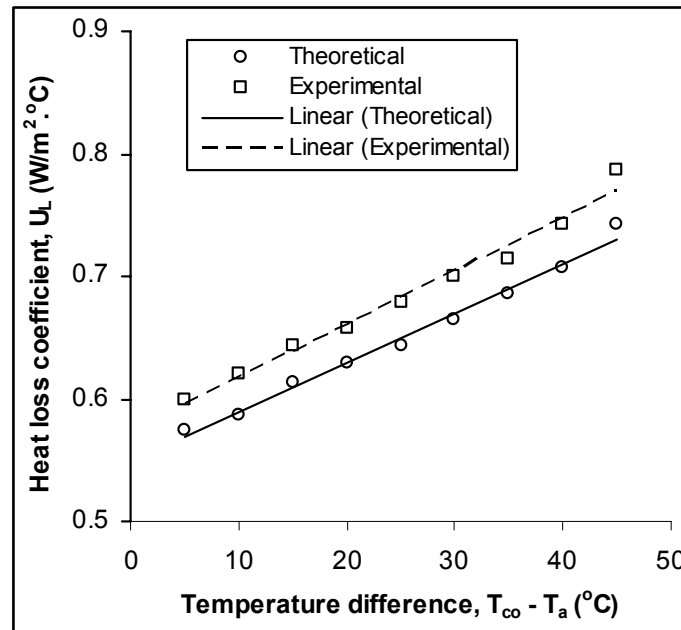


Figure 4 A typical day hourly variation of ambient temperature, collector-outlet water temperature and solar radiation.

The curves of theoretical and experimental heat loss coefficients of the collector as a function of the temperature difference between the collector outlet water temperature ( $T_{co}$ ) and the ambient temperature ( $T_a$ ) are shown in **Figure 5**. The heat loss coefficient varies with the temperature difference; it increases as the temperature difference increases. The increase in temperature difference between the collector and the ambient temperature increases the rate at which heat is lost from the system. The heat loss coefficient of the

collector varies from 0.58 to 0.79  $W/m^2 \cdot ^\circ C$  when the temperature difference is between 5 and 45  $^\circ C$ . The theoretical results agreed well with the experimental results, but slight higher deviations of experimental values were obtained. The discrepancies were possibly due to the computational assumptions presumed and the accuracy of the measurements. The average heat loss coefficient of 0.68  $W/m^2 \cdot ^\circ C$  obtained from experimental results is 4.4 % higher than 0.65  $W/m^2 \cdot ^\circ C$  obtained in the theoretical analysis.



**Figure 5** Heat loss coefficients of the collector as a function of temperature difference between collector outlet water and ambient air temperatures ( $T_{co} - T_a$ ).

Theoretical and experimental results of variation of useful heat rate of the solar collector with time are shown in **Figure 6**. As shown in this figure, the useful heat rate is at its maximum around mid-day when the collector receives the highest energy, but it is low in the morning and late afternoon due to the low solar radiation during this period. As expected, comparing **Figure 4** with **Figure 6** the useful heat rate is a function of solar

radiation; increase in solar radiation increases the useful heat rate obtained from the collector. In addition, the difference observed between the theoretical and experimental results in the morning and late afternoon is due to the angle of incidence of the sun during these periods, which impairs the operation of the collector. Beside this, the theoretical results agreed well with the experimental results.

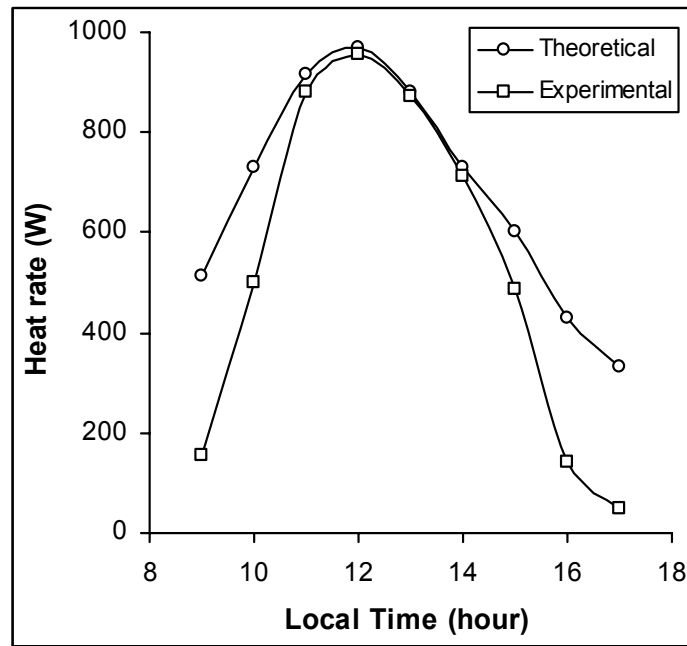


Figure 6 Variation of useful heat rate of the solar collector with time.

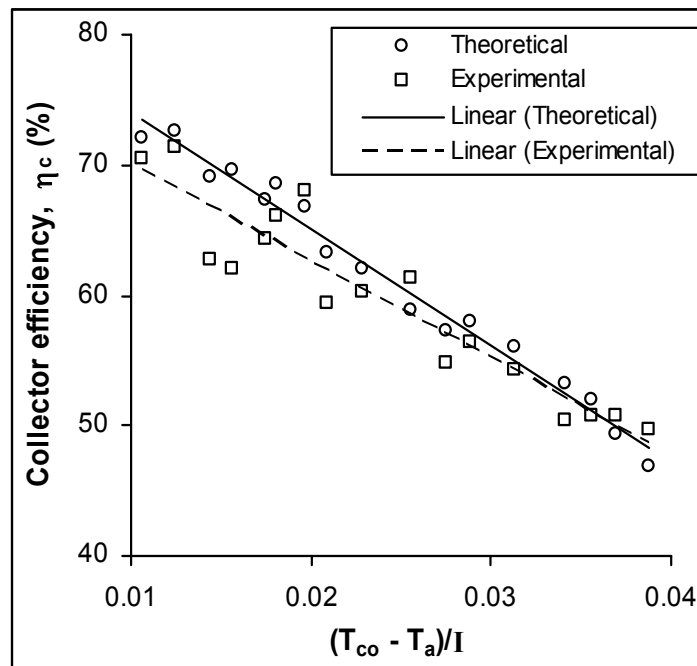
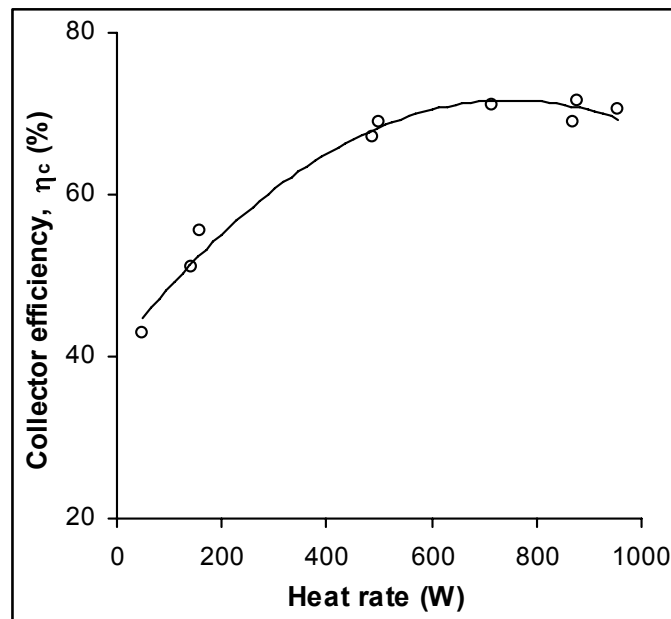


Figure 7 Collector efficiency versus collector performance coefficient  $(T_{ci} - T_a)/I$ .

The variation of the collector efficiency with the collector performance coefficient  $(T_{ci} - T_a)/I$  is shown in **Figure 7**. As shown in this figure, the collector efficiency reduces as the collector performance coefficient increases. Increase in the temperature difference  $(T_{ci} - T_a)$  will increase both the collector performance coefficient and the heat losses from the collector, which reduces the collector efficiency. The curves also show a good agreement between the theoretical and

experimental results. **Figure 8** shows the experimental efficiency of the solar collector as a function of heat rate. The collector performance improves with an increase in heat rate until it reaches its maximum value after which any additional increase in the heat rate has no effect on the performance of the solar collector. During the test a maximum efficiency of 72.2 % was obtained at optimum heat rate of 785 W.



**Figure 8** Variation of efficiency with heat rate of the solar collector.

### Conclusion

This paper analyses theoretically and experimentally, the heat transfer in a flat-plate absorber solar collector with water tubes spreading across its width. The system was tested and its thermal performance was evaluated. The results obtained show that the maximum temperature occurred after the peak solar radiation. During the test, a maximum water temperature of 83.5 °C was obtained, while the maximum ambient temperature for the day was 34.5 °C. The collector efficiency is high especially around mid-day when the collector receives the highest energy and the useful heat rate is at a maximum.

The heat loss coefficient varies slightly with the temperature difference. It increases as the temperature difference increases. The theoretical results agreed well with the experimental results, except that a slightly higher deviation of heat loss was obtained in the experimental analysis. Also deviations were observed in the morning and late afternoon due to the large angle of incidence of the sun that resulted in low solar radiation during these periods. The average heat loss coefficient of 0.68  $W/m^2 \cdot ^\circ C$  obtained from experiments is 4.4 % higher than 0.65  $W/m^2 \cdot ^\circ C$  obtained in the theoretical analysis. The results reveal that the performance of the solar collector depends much on the heat rate. The collector efficiency increases

as the heat rate increases until a maximum value is reached. During the test, the maximum efficiency obtained was 72.2 % at an optimum heat rate of 785 W.

### References

- [1] R Kumar and MA Rosen. A critical review of photovoltaic-thermal solar collectors for air heating. *Appl. Energ.* 2011; **88**, 3603-14.
- [2] MA Eltawil and DVK Samuel. Vapour compression cooling system powered by solar pv array for potato storage. *Agric. Eng. Inter.: CIGR Journal* 2007; **9**, 1-23.
- [3] C Lamnatou, E Papanicolaou, V Belessiotis and N Kyriakis. Experimental investigation and thermodynamic performance analysis of a solar dryer using an evacuated-tube air collector. *Appl. Energ.* 2012; **94**, 232-43.
- [4] DEFRA. Department for Environment Food and Rural Affairs. New Bill and strategy lay foundations for tackling climate change, Available at: <http://www.defra.gov.uk/environment/climatechange/uk/legislation/index.html>, accessed July 2008.
- [5] C Garnier, J Currie and T Muneer. Integrated collector storage solar water heater: Temperature stratification. *Appl. Energ.* 2009; **86**, 1465-9.
- [6] A Alvarez, O Cabeza, MC Muniz and LM Varela. Experimental and numerical investigation of a flat-plate solar collector. *Energ.* 2010; **35**, 3707-16.
- [7] BO Bolaji and AP Olalusi. Performance evaluation of a mixed-mode solar dryer. *AU J. Tech.* 2008; **11**, 225-31.
- [8] M Thirugnanasambandam, S Iniyan and R Goic. A review of solar thermal technologies. *Renew. Sustain. Energ. Rev.* 2010; **14**, 312-22.
- [9] VB Vaidya, PV Walke and VM Kriplani. Effects of wind shield on performance of solar flat plate collector. *Int. J. Appl. Eng. Res.* 2011; **6**, 379-89.
- [10] AME Momin, TS Saini and SC Solanki. Heat transfer and friction in solar air heater duct with v-shaped rib roughness on absorber plate. *Int. J. Heat Mass Tran.* 2002; **45**, 3383-96.
- [11] J Huang, S Pu, W Gao and Y Que. Experimental investigation on thermal performance of thermosyphon flat-plate solar water heater with a mantle heat exchanger. *Energ.* 2010; **35**, 3563-8.
- [12] BO Bolaji. Mathematical modelling and experimental investigation of collector efficiency of a thermosyphonic solar water heating system. *Analele Universitatii Eftimie Murgu* 2011; **28**, 55-66.
- [13] R Tang, Y Cheng, M Wu, Z Li and Y Yu. Experimental and modeling studies on thermosyphon domestic solar water heaters with flat-plate collectors at clear nights. *Energ. Convers. Manag.* 2010; **51**, 2548-56.
- [14] H Taherian, A Rezanian, S Sadeghi and DD Ganji. Experimental validation of dynamic simulation of the flat plate collector in a closed thermosyphon solar water heater. *Energ. Convers. Manag.* 2011; **52**, 301-7.
- [15] M Rommel and W Moock. Collector efficiency factor for absorbers with rectangular fluid ducts. *Sol. Energ.* 1997; **60**, 199-207.
- [16] KAR Ismail and MM Abogderah. Performance of a heat pipe solar collector. *J. Sol. Energ. Eng.* 1998; **120**, 51-9.
- [17] JA Duffie and WA Beckman. *Solar Engineering of Thermal Processes*. 2<sup>nd</sup> ed. John Wiley and Sons, New York, 1991.
- [18] J Facao and AC Oliveira. Analysis of a flat-plate heat pipe solar collector. In: *Proceedings of International Conference on Sustainable Energy Technologies*, Nottingham, UK. 2004, p. 1-5.
- [19] BO Bolaji. Exergetic analysis of solar drying systems. *Nat. Resour.* 2011; **2**, 92-7.
- [20] BO Bolaji. Flow design and collector performance of a natural circulation solar water heater. *J. Eng. Appl. Sci.* 2006; **1**, 7-13.